© 2019. Published by The Company of Biologists Ltd | Development (2019) 146, dev177527. doi:10.1242/dev.177527

RESEARCH REPORT

Wheat AGAMOUS LIKE 6 transcription factors function in stamen development by regulating the expression of *Ta APETALA3*

Yali Su[1,*], Jinxing Liu[2,*], Wanqi Liang[3], Yanhua Dou[1], Ruifeng Fu[3], Wenqiang Li[1], Cuizhu Feng[1], Caixia Gao[2], Dabing Zhang[3], Zhensheng Kang[4,‡] and Haifeng Li[1,‡]

ABSTRACT

Previous studies have revealed the functions of rice and maize *AGAMOUS LIKE 6* (*AGL6*) genes *OsMADS6* and *ZAG3*, respectively, in floral development; however, the functions of three wheat (*Triticum aestivum*) *AGL6* genes are still unclear. Here, we report the main functions of wheat *AGL6* homoeologous genes in stamen development. In RNAi plants, stamens showed abnormality in number and morphology, and a tendency to transform into carpels. Consistently, the expression of the B-class gene *TaAPETALA3* (*AP3*) and the auxin-responsive gene *TaMGH3* was downregulated, whereas the wheat ortholog of the rice carpel identity gene *DROOPING LEAF* was ectopically expressed in RNAi stamens. TaAGL6 proteins bind to the promoter of *TaAP3* directly. Yeast one-hybrid and transient expression assays further showed that TaAGL6 positively regulates the expression of *TaAP3 in vivo*. Wheat AGL6 transcription factors interact with TaAP3, TaAGAMOUS and TaMADS13. Our findings indicate that TaAGL6 transcription factors play an essential role in stamen development through transcriptional regulation of *TaAP3* and other related genes. We propose a model to illustrate the function and probable mechanism of this regulation. This study extends our understanding of *AGL6* genes.

KEY WORDS: Wheat, *AGAMOUS LIKE 6*, Stamen, *APETALA3*, MADS-box, Flower

INTRODUCTION

Flower development is the basis for seed development in angiosperms. On the basis of analyses of flower mutants in the model dicot species *Arabidopsis thaliana* and *Antirrhinum majus*, the ABCDE model was proposed to interpret the molecular mechanism underlying flower development (Coen and Meyerowitz, 1991; Pelaz et al., 2000; Theißen, 2001; Ditta et al., 2004).

In rice (*Oryza sativa*), the functions of many floral genes have been elucidated. These genes included *OsMADS14*, *OsMADS15* and *OsMADS18* (Kobayashi et al., 2012; Wu et al., 2017), B class gene *OsMADS16/SPW1* (Nagasawa et al., 2003), C class genes *OsMADS3* and *OsMADS58* (Yamaguchi et al., 2006; Dreni et al., 2011; Hu et al., 2011), D class gene *OsMADS13* (Dreni et al., 2007; Li et al., 2011b), E class genes *OsMADS7* and *OsMADS8* (Cui et al., 2010), *OsMADS1* (Jeon et al., 2000), *OsMADS34* (Gao et al., 2010; Kobayashi et al., 2010; Lin et al., 2014), and carpel identity gene *DROOPING LEAF* (*DL*) (Yamaguchi et al., 2004; Li et al., 2011b).

In the *MADS-box* gene family, *AGAMOUS LIKE 6* (*AGL6*) genes constitute an ancient sub-family of *MADS-box* genes and can be found extensively in the plant kingdom (Becker and Theissen, 2003; Reinheimer and Kellogg, 2009). Two *AGL6* genes have been identified in *Arabidopsis*: *AGL6* and *AGL13*. Because of probable functional redundancy, null mutant plants of *agl6-2* showed no obvious phenotypes in flowering time and floral development (Koo et al., 2010). Analyses of transgenic *Arabidopsis* overexpressing *AGL6* showed its function in flowering time (Koo et al., 2010; Yoo et al., 2011b). Additionally, *AGL6* functions in leaf movement and is involved in the formation of the axillary bud (Yoo et al., 2011a; Huang et al., 2012). *AGL13* regulates the development of male and female gametophytes (Hsu et al., 2014).

In *Petunia*, *pMADS4*/*PhAGL6* showed redundant functions with E class genes *FBP2* and *FBP5* (Rijpkema et al., 2009). In grasses, the maize (*Zea mays*) *AGL6* gene *ZAG3* regulates the development of floral organs and meristems (Thompson et al., 2009). Rice *OsMADS6* affects the development of paleas, lodicules, stamens and ovules, as well as the floral meristems (FMs) and seeds (Ohmori et al., 2009; Li et al., 2010; Zhang et al., 2010; Duan et al., 2012). Analyses of genetic interactions between *OsMADS6* and other floral genes indicated that *OsMADS6* is a master floral regulator (Li et al., 2011a).

The bread wheat (*Triticum aestivum*) is a hexaploid plant (Shewry, 2009). Although an ABCDE model has been proposed for wheat (Murai, 2013), the biological functions of most wheat floral genes have not yet been elucidated.

Previous studies have shown that *TaMADS12* and *TaAGL37* are *AGL6* homologues in wheat (Paolacci et al., 2007; Reinheimer and Kellogg, 2009). In this study, we have investigated the functions of wheat *AGL6* homoeologous genes. Our results show that TaAGL6 transcription factors play an essential role in stamen development through the transcriptional regulation of *TaAP3*.

RESULTS AND DISCUSSION

Wheat genome has three *AGL6* homoeologous genes

For the sake of cloning the full cDNAs of *TaAGL6*, 3′ and 5′ rapid amplification of cDNA ends (RACE) experiments were performed (Table S1). About 1000 bp and 400 bp PCR products in which 205 bp overlapped were obtained (Fig. S1A) and cloned into T vectors. Sequencing results showed that both 3′ and 5′ RACE products included three conserved but distinctive sequences (Fig. S1B), indicating that there are three homoeologous *TaAGL6* genes, which is consistent with the wheat genome (Appels et al., 2018).

[1]State Key Laboratory of Crop Stress Biology for Arid Areas and College of Agronomy, Northwest A&F University, Yangling 712100, China. [2]Institute of Genetics and Developmental Biology, Chinese Academy of Sciences, Beijing 100101, China. [3]School of Life Sciences and Biotechnology, Shanghai Jiao Tong University, Shanghai 200240, China. [4]State Key Laboratory of Crop Stress Biology for Arid Areas and College of Plant Protection, Northwest A&F University, Yangling, Shaanxi, 712100, China.
*These authors contributed equally to this work

‡Authors for correspondence (lhf@nwsuaf.edu.cn; kangzs@nwsuaf.edu.cn)

Z.K., 0000-0002-5863-6218; H.L., 0000-0002-4046-6855

Received 3 March 2019; Accepted 11 September 2019

Development (2019) 146, dev177527. doi:10.1242/dev.177527

According to chromosome locations, they were named as *TaAGL6-A*, *TaAGL6-B* and *TaAGL6-D*. *TaAGL6-A* corresponds to reported *TaMADS37* and *TaAGL6-B* corresponds to *TaMADS12*. Every cDNA includes an open reading frame and encodes one AGL6 protein (Fig. S2). In addition to MADS-box and K domains, these proteins have AGL6 motifs I and II (Fig. S2). They were classified into the grass AGL6-I-ZAG subgroup (Dreni and Zhang, 2016). Although some SNPs resulted in some differences in the protein sequence, they did not significantly affect the functions, according to the prediction with the software Protein Variation Effect Analyzer (Fig. S2B). These results indicate that they have similar functions.

TaAGL6 genes display conserved expression patterns

First, we analyzed *TaAGL6* gene expression pattern using quantitative RT-PCR with primers simultaneously applicable for *TaAGL6-A*, *TaAGL6-B* and *TaAGL6-D*. Consistent with a previous report (Feng et al., 2017), results showed that *TaAGL6* genes are strongly expressed in the inflorescences from stage 3-8.5 (Fig. 1A,B), according to previous classification (Waddington et al., 1983). The transcripts mainly accumulate in the paleas, lodicules and pistils at stage 6-7. Relatively, the expression in the lemmas and stamens is very low (Fig. 1C). In addition, qRT-PCR with specific primers showed that these three *TaAGL6* genes have similar expression patterns in the floral organs (Fig. S3).

We further performed *in situ* hybridization. *TaAGL6* mRNA was not detected in the inflorescences at stage 2 (Fig. 1D), and the transcripts first emerged in the FMs at stage 3 (Fig. 1E) and then in the palea and lodicule primordial at stage 3.5-4 (Fig. 1F,G). *TaAGL6* mRNA was then continually detected in the developing lodicules and paleas at stage 4-7.5 (Fig. 1H-P). Meanwhile, *TaAGL6* transcripts were detected in the carpels and ovules at stage 4.5-7.5 (Fig. 1I-P), while signal in the lemmas and stamens was undetectable (Fig. 1I,K-P). When hybridized with sense probes, no signal was found (Fig. 1Q).

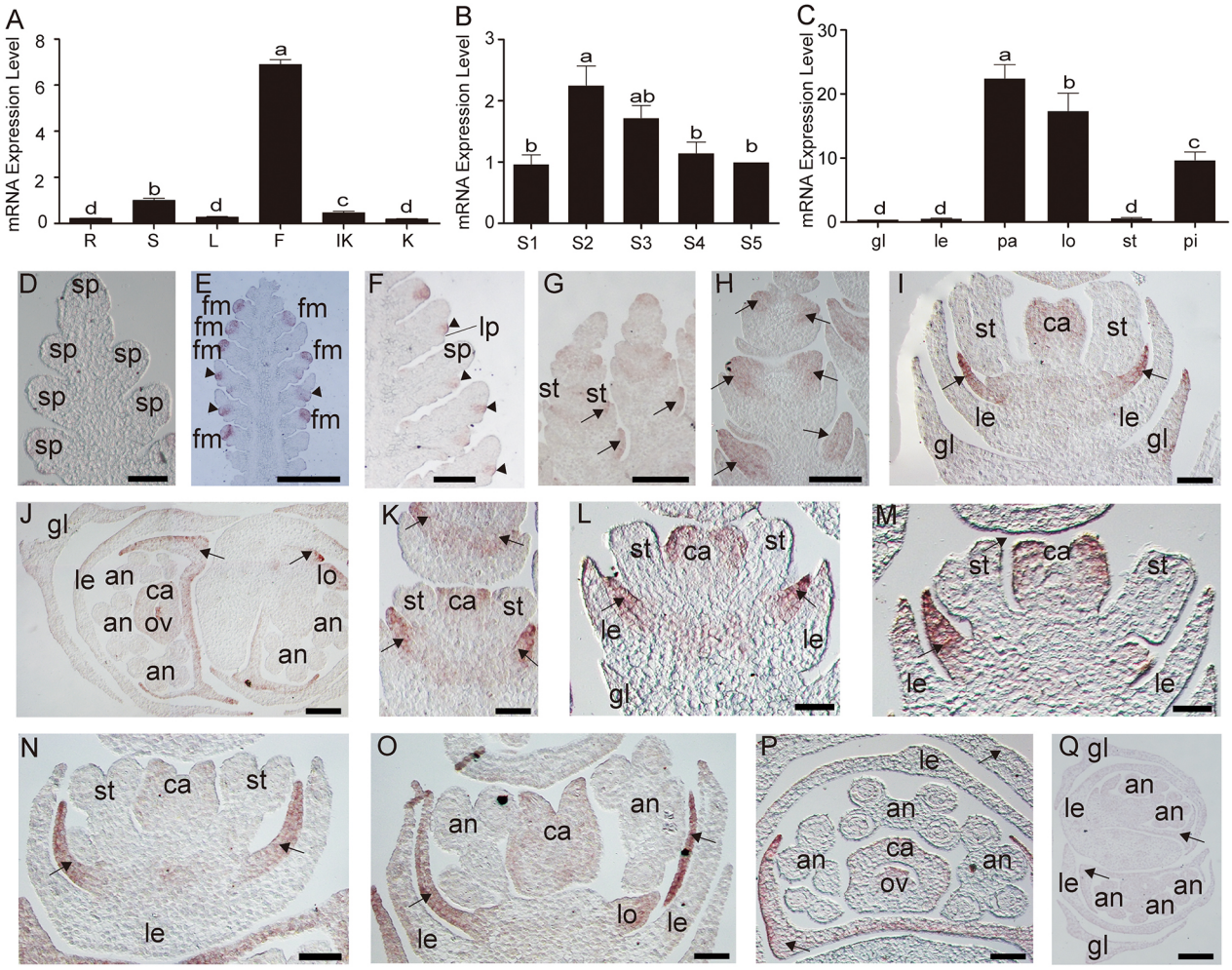

Fig. 1. Expression profile of *TaAGL6* genes. (A) The expression of *TaAGL6* in roots (R), stems (S), leaves (L), flowers (F), immature kernels (IK) and mature kernels (MK). (B) The expression of *TaAGL6* in inflorescences or florets at different stages. S1-S5, inflorescences at stages 3-3.25, 3.25-3.5, 4-5.5, 6-7 and 7.5-8.5, respectively. (C) The expression of *TaAGL6* genes in the glumes (gl) and floral organs at stage 6-7. le, lemma; pa, palea; lo, lodicule; st, stamen; pi, pistil. Data are mean±s.d. a-d indicate significant differences (P<0.05 by Student's t-test). (D-Q) Results of mRNA *in situ* hybridization. (D) No signal in one inflorescence at stage 2. (E) The transcripts of *TaAGL6* in FMs at stage 3. (F) Signals in lodicule primordia at stage 3.5. (G,H) The transcripts of *TaAGL6* accumulated in the palea primordia and paleas at stage 4. (I) Signals in the carpel primordium at stage 5. (J) The global expression pattern in florets at stage 6.5-7. (K-O) Wheat floret longitudinal sections to show that *TaAGL6* mRNA signal accumulated in the paleas, lodicules, carpels and ovules. No obvious signal was detected in the stamens or anthers. (K,L) Stage 4.25 to 4.5; (M,N) stage 5.5; (O) stage 7. (P) One transverse section of a floret at stage 7.5. (Q) Negative control. A floret at stage 7 hybridized with sense probes. sp, spikelet; fm, FM; lp, lemma primordium; st, stamen; gl, glume; le, lemma; ca, carpel; lo, lodicule; ov, ovule; an, anther. Lodicule primordia are indicated by arrowheads; paleas are indicated by arrows. Scale bars: 20 µm in F; 100 µm in D,G,K,Q; 200 µm in H; 500 µm in E,I,J,L-P.

Development (2019) 146, dev177527. doi:10.1242/dev.177527

Overexpressing *TaAGL6* genes promotes early flowering

TaAGL6 genes were overexpressed in *Arabidopsis*. Generally, the transgenic plants harboring different *TaAGL6* genes showed similar phenotypes that could be classified into two types: early flowering and dwarf (Fig. S4A-E); and with an increased number of stems or branches (Fig. S4F-J). Relatively, the expression level of the target gene was higher in the early flowering lines than in the multi-branch lines (Fig. S5A). These observations further indicate that three *TaALG6* genes have similar functions.

FLOWERING LOCUS T (*FT*) in *Arabidopsis* is a master flowering regulator (Gu et al., 2013). We analyzed the expression of *FT* in our transgenic plants. The expression level of *FT* is higher in the transgenic lines than the control during the vegetative stage, consistent with the early flowering phenotype (Fig. S4K).

We also generated transgenic wheat overexpressing *TaAGL6-B* and obtained 27 positive lines. The expression level of the target gene was increased in most lines, especially in lines 18 and 30 (Fig. S5B). The flowering time of 12 lines was 10-20 days earlier than that of the control (Fig. S6A–E), and the expression of wheat *FT* homologs was upregulated in the transgenic wheat (Fig. S6F); however, no floral phenotype was observed.

TaAGL6 genes function in stamen development

Because all three *TaAGL6* genes are expressed in the flowers and showed similar functions in transgenic *Arabidopsis*, we speculated that their functions are redundant. Therefore, we knocked down these *TaAGL6* genes simultaneously using RNA interference (RNAi). A total of 21 transgenic wheat lines were obtained. qRT-PCR results showed that the expression of *TaAGL6* genes in lines 17-2, 28-3 and 3-2 was decreased drastically (Fig. S5C), so they were selected for further analyses. At the vegetative stage, none of them showed obvious phenotypes. At the reproductive stage, abnormal floral phenotypes were observed.

In about 30% of RNAi florets, stamens display abnormality in the number or/and the morphology. One normal floret generates three stamens (Fig. 2A), whereas some transgenic florets bear only two stamens (Fig. 2B). The morphology of some RNAi stamens was also affected (Fig. 2C,D). As shown in Fig. 2E, a normal stamen has four anther cavities; however, in some transgenic stamens, two anther cavities fuse together or one stamen has only two anther cavities (Fig. 2F,G). The vigor of pollen grains was affected in all RNAi stamens, irrespective of morphology (Fig. 2H-J). As a result, the seed-setting rate is lower (35.81%) than the control (96.34%) (Fig. 2K). Occasionally, some florets displayed strong phenotypes by generating three or four carpels without stamens or with anther-stigma mosaic organs (Fig. 2L-N).

Scanning electron microscope (SEM) observation showed the developmental defects of stamens at the early stage, which is consistent with these phenotypes. In normal cases, three stamen primordia are formed; however, in some transgenic florets, only two normal stamen primordia were observed (Fig. 2O,P). In addition, all stamens in the wild type are quadrangular; however, in some transgenic florets, only one stamen was quadrangular and the morphology of the other two stamens was not normal (Fig. 2Q,R). These phenotypes were observed in not only T_0 plants but also T_1 and T_2 plants.

Because only a single *AGL6* gene was found in the wheat A, B and D sub-genome, and these homoeologous genes are mainly expressed in the paleas and lodicules, we predicted that wheat *AGL6* genes function as rice OsMADS6 genes, and also play roles in paleas and other organs.

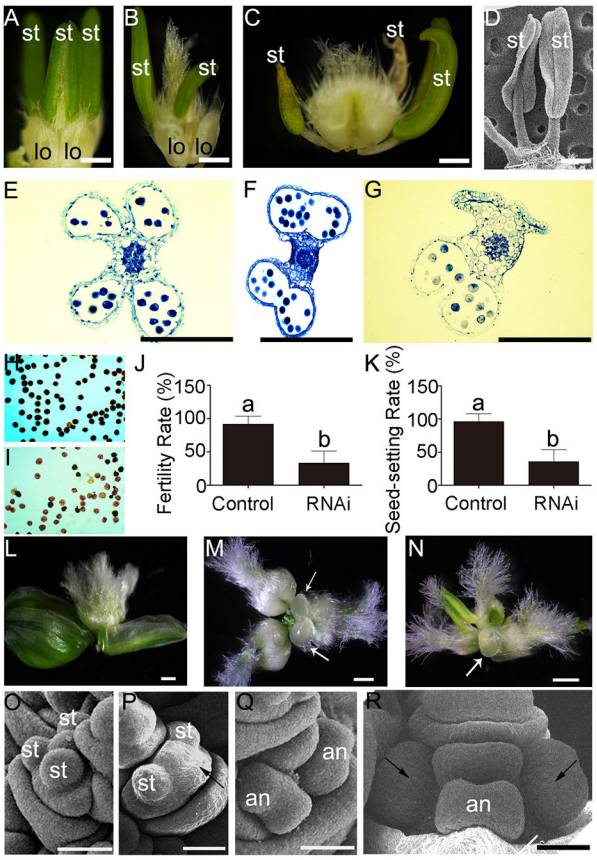

Fig. 2. Phenotypes of *TaAGL6* RNAi stamens. (A) One wild-type floret with three stamens. (B) One RNAi floret with a normal and abnormal stamen. (C) One RNAi floret with three abnormal stamens. The lemmas and paleas were removed in A-C. (D) Scanning electron micrograph of abnormal RNAi stamens. (E-G) Histological analyses of wild-type (E) and abnormal RNAi anthers (F,G). (H,I) Wild-type (H) and RNAi pollen grains (I) stained with I_2-KI. (J) Fertility rate of pollen grains. (K) Seed-setting rate. (L-N) RNAi florets showing strong phenotypes (arrows indicate lodicules). The lemmas and paleas in M and N were removed. (O) Scanning electron micrograph of one wild-type floret with three stamen primordia. (P) Scanning electron micrograph of one RNAi floret with two stamen primordia. (Q) Scanning electron micrograph of one wild-type floret to show the quadrangular stamens. (R) Scanning electron micrograph of one RNAi floret to show two irregular stamens (indicated by black arrows). an, anther; st, stamen; lo, lodicules. In J and K, data are mean±s.d. Values in J and K were obtained from 30 replications (n=30); a and b indicate the significant differences according to Student's t-test (P<0.05). Scale bars: 100 µm in A-C; 20 µm in E-G; 50 µm in D,L-N; 500 µm in O-R.

Surprisingly, no obvious phenotype was observed in RNAi paleas and lodicules. Reinheimer and Kellogg (2009) proposed that the expression of grass *AGL6* genes in the ovule is conserved, whereas the expression domain of the palea is acquired during the evolution process. *TaAGL6* genes might acquire the expression domain in the paleas, but have no functions in palea development. During the evolution process, the functions of *AGL6* become divergent, and *OsMADS6* gains the function of specifying palea identity. Another possibility is that the low expression of TaAGL6 genes in RNAi lines is enough to maintain normal palea and lodicule development.

TaAGL6 transcription factors interact with other floral regulators

Several AGL6 transcription factors interact with floral regulators. ZAG3 forms a heterodimer with C-function protein ZAG1

Development (2019) 146, dev177527. doi:10.1242/dev.177527

(Thompson et al., 2009); OsMADS6 interacts with D-function protein OsMADS13 (Li et al., 2011a); and OsMADS6 and OsMADS17 form protein complexes with B-function proteins (Seok et al., 2010). Similar to the E-function protein FBP2, petunia AGL6 interacts with C- and D-function proteins (Rijpkema et al., 2009). These and other results indicate that AGL6 transcription factors have partial E-function proteins.

To clarify whether TaAGL6 proteins interact with other floral regulators, yeast two-hybrid (Y2H) and bimolecular fluorescence complementation (BiFC) assays were performed. The results showed that TaAGL6-A interact with TaAP3, TaAG and TaMADS13 not only in yeast cells, but also in tobacco (*Nicotiana benthamiana*) leaf cells (Fig. 3A,B). We further verified these interactions *in planta* by performing co-immunoprecipitation (Fig. 3C). In addition, TaAGL6-A displayed transcription activity, whereas TaAP3, TaAG and TaMADS13 did not (Fig. S7). Meanwhile, TaAGL6-B and TaAGL6-D interact with TaAP3, TaAG and TaMADS13 in yeast cells and tobacco leaf cells (Fig. S8). These results showed that TaAGL6 proteins act as E-class transcription factors, and further implied redundant functions.

TaAGL6 transcription factors regulate stamen development by targeting *TaAP3* directly

Previously, we investigated the expression patterns of *TaAP3*, *TaAG*, *TaDL*, *TaMADS13*, *TaSEP* and *TaLHS1* in floral organs (Li et al., 2016). We analyzed the expression of related genes in *TaAGL6* RNAi stamens. qRT-PCR results showed that the expression of *TaAP3* and *TaMGH3* is obviously decreased in RNAi stamens. The ectopic expression of *TaDL*, *TaMADS13* and *TaLHS1* was detected, whereas the expression of *TaAG* and *TaMADS58* is slightly increased in the RNAi stamens (Fig. S9). These results further verified the developmental defects in *TaAGL6* RNAi stamens at the molecular level.

OsMGH3 is an auxin-responsive gene and is regulated by *OsMADS6* indirectly; it also functions in flower development (Zhang et al., 2010; Yadav et al., 2011). We screened the promoters of three *TaMGH3* genes but no CArG motif was found. Therefore, they are indirect downstream genes of *TaAGL6*. In wheat, two *TaAP3* homoeologous genes exist: *TaAP3-B* and *TaAP3-D*. In the promoters of *TaAP3-B* and *TaAP3-D*, two CArG motifs were found, respectively (Fig. 4A). Taking the transcription activity of TaAGL6 proteins into account, we wondered whether TaAGL6 transcription factors regulate the expression of *TaAP3* directly. Therefore, we expressed and purified the TaAGL6-B-GST fusion protein (Fig. 4B, C) for electrophoresis mobility shift assays (EMSAs). The EMSA results showed that the fusion protein could bind to motif 1 (Fig. 4D), but it could not bind to the other three motifs (Fig. S10). Results of yeast one hybrid (Y1H) further verified the interactions between three TaAGL6 transcription factors and M1 (Fig. 4E,F). Transient expression assay further showed the positive regulation of TaAGL6 to *TaAP3-B in planta* (Fig. 4G,H).

As transcription factors, MADS-box proteins function through transcriptional regulation of target genes. In addition to regulating the expression of *OsMGH3* indirectly (Zhang et al., 2010), *OsMADS6* regulates the expression of *OsMADS58* and *OsFDML1* directly (Li et al., 2011b; Tao et al., 2018). However, we failed to identify the ortholog of *OsFDML1* in the wheat genome (data not shown). These results indicate that the detailed mechanism is different.

Mutations of *AP3* resulted in the homeotic transformation of stamens to carpels. Similar phenotypes were observed in *Antirrhinum majus defa*, maize *Silky1* and rice *spw1* mutant

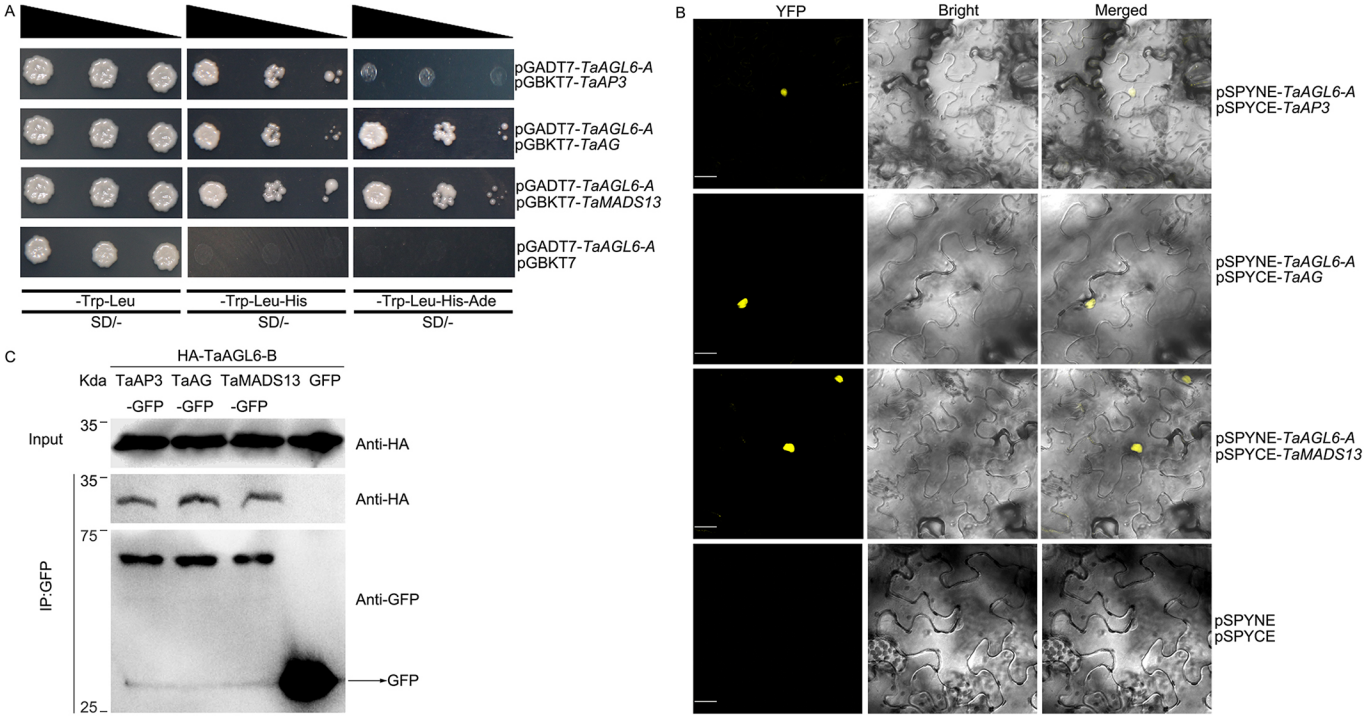

Fig. 3. Interactions between TaAGL6 and wheat floral regulators. (A) Results of Y2H analyses to show interactions between TaAGL6 and TaAP3, TaAG and TaMADS13. (B) BiFC analyses to show the interactions in tobacco leaf cells (left, YFP; middle, bright field; right, merged). (C) Results of co-immunoprecipitation. The co-expressed HA-TaAGL6 and TaAP3-GFP, TaAG-GFP, TaMADS13-GFP and GFP proteins were immunoprecipitated with GFP-Trap MA beads, and detected using anti-GFP and -HA antibodies. Three replicates were performed for every experiment.

Development (2019) 146, dev177527. doi:10.1242/dev.177527

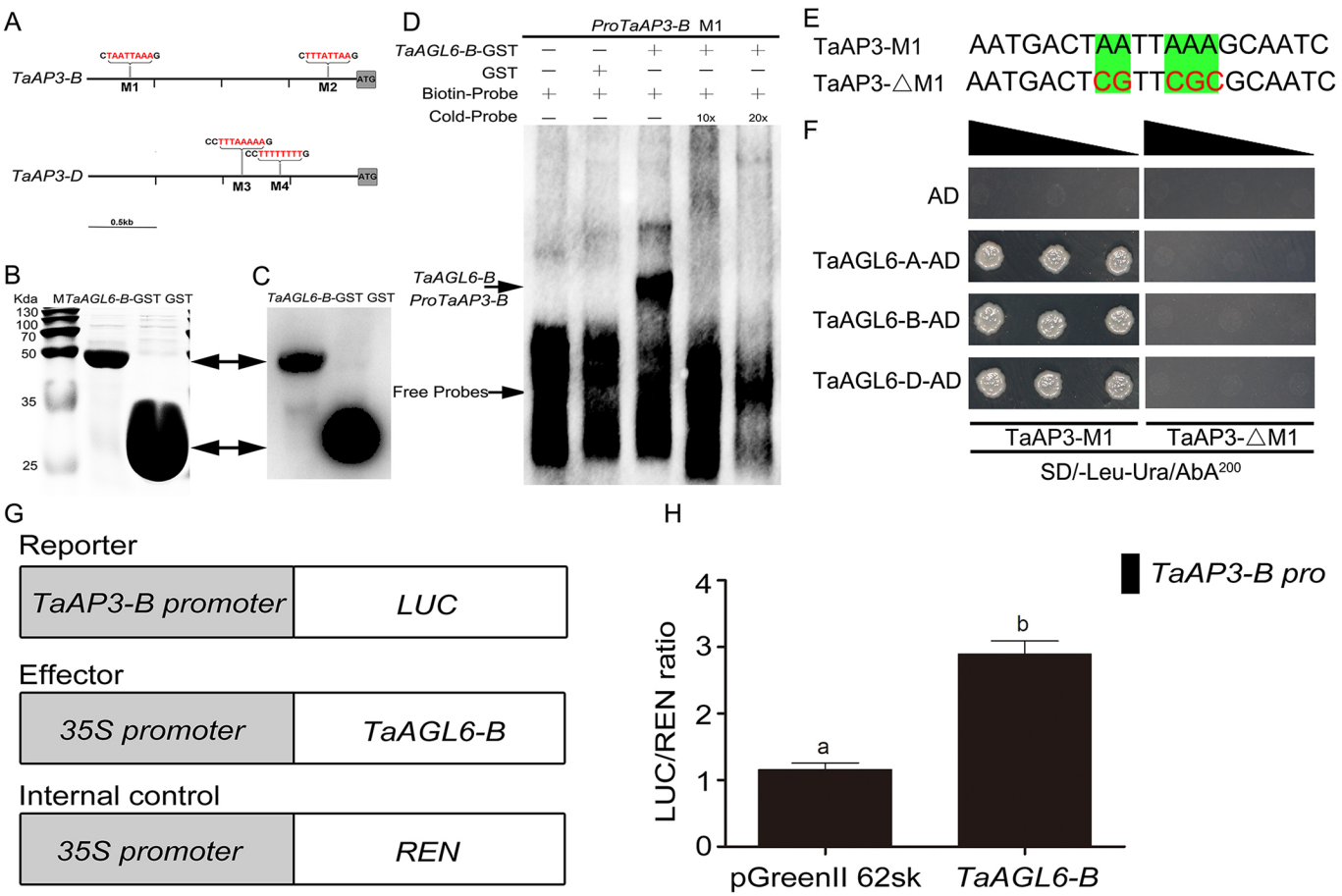

Fig. 4. Positive regulation of TaAP3-B by TaAGL6 proteins. (A) CArG motifs in *TaAP3-B* and *TaAP3-D* promoters. (B) The purified TaAGL6-B-GST protein and GST. (C) Western blotting analysis of *TaAGL6*-B-GST protein and GST. (D) EMSA results. (E) M1 and mutated M1. The motif is indicated in green and the mutated bases are indicated in red. (F) Y1H results showing the binding of TaAGL6 proteins to M1. pGADT7 vector is used as negative control. (G) Schematic of the reporter and effecter. (H) Relative reporter activity (LUC/REN) in tobacco leaves expressing the indicated reporter and effecter. Data are mean±s.d. obtained from three replications. Different letters indicate a significant difference (P<0.05 by Student's t-test).

plants (Schwarz-Sommer et al., 1990; Ambrose et al., 2000; Nagasawa et al., 2003; Whipple et al., 2004), suggesting important and conserved functions for *AP3* genes during stamen development.

The disrupted expression of *AP3* in *TaAGL6* RNAi stamens may be the cause of abnormality in stamen development (Fig. 2). In addition, *SPW1* represses the expression of *DL* (Nagasawa et al., 2003). This mechanism might be conserved in wheat (Murai, 2013). Consistent with this prediction, *TaDL* is ectopically expressed in *TaAGL6* RNAi stamens, accompanied with deceased expression of *TaAP3* (Fig. S9), indicating the potential homeotic transformation from stamens to carpels. The ectopic expression of *TaLHS1* and *TaMADS13* (Fig. S9) and the severe phenotypes (Fig. 2) further support this prediction.

In general, our results extended understanding of *AGL6* genes and provided further evidence that AGL6 proteins have E-functions. Moreover, our findings indicate the distinctive functions and mechanisms of action of *TaAGL6* genes in stamen development. We propose a model to illustrate these findings (Fig. S11) but further studies will help us to reveal the mechanism.

MATERIALS AND METHODS

Plant materials and growth conditions

The wheat varieties Chinese Spring (CS) and Kenong199 (KN199) were used in this study. They were planted in a glasshouse under a photoperiod of 12 h of light at 22°C and 12 h of darkness at 16°C, or in an isolated experimental field under natural conditions at the Northwest A&F University (108°4′E, 34°15′N). The *Arabidopsis* ecotype Columbia-0 (Col-0) was used to generate the transgenic lines in growth chambers with a light period of 16 h and dark period of 8 h at 23°C. Phenotypes were observed in the T2 and T3 plants. Tobacco was planted under the same growth conditions as those of *Arabidopsis*.

RACE

Total RNA was extracted from CS flowers, and the SMART RACE kit (TaKaRa) was used to synthesize the cDNA and generate the 5′-RACE and 3′-RACE products, according to the protocol. The specific primers for 5′-RACE (5GSP in Table S1) and 3′-RACE (3GSP in Table S1) were designed by Primer Premier 5.0. Specific PCR products were cloned into the pMD-19T vector (TaKaRa) and different positive clones were sequenced.

Quantitative RT-PCR

The roots, stems, leaves and flowers of wheat were collected at the heading stage. Inflorescences at different stages were collected and judged according to a previous study (Waddington et al., 1983). Glumes and different floral organs were collected from florets at stages 6-7. Total RNAs were extracted from different organs using TRIzol reagent (Sangon Biotech), according to the manufacturer's instructions. cDNAs were synthesized with AMV reverse transcriptase (Roche). qRT-PCR was performed using TB Green Premix Ex TaqII (TaKaRa) and CFX96 real-time PCR detection system (Bio-Rad). Three technical and three biological replicates were used. The data were analyzed using the $2^{-\Delta\Delta CT}$ method (Livak and Schmittgen, 2001). The common primers were designed according to the consensus sequences,

Development (2019) 146, dev177527. doi:10.1242/dev.177527

while the specific primers (TaAGL6AF/TaAGL6AR, TaAGL6BF/TaAGL6BR and TaAGL6DF/TaAGL6DR) for analyzing the expression of every *TaAGL6* gene were designed according to the differences between the full cDNA sequences, specifically a 5 bp insertion into the 5′ UTR of *TaAGL6-A*, and a 9 bp deletion in the 3′UTR of *TaAGL6-D*. The specificity of each pair of primers was verified by sequencing the RT-PCR products (data not shown). The primers are listed in Table S1.

In situ hybridization

CS inflorescences at different stages were fixed in FAA (50% ethanol, 5% acetic acid and 3.7% formaldehyde) overnight at 4°C. The materials were then treated and the experiments were performed as described previously (Li et al., 2011b; Tao et al., 2018). The probes labeled with digoxigenin were prepared using the *in vitro* transcription kit (Roche), according to the protocol and previous studies (Li et al., 2011b; Tao et al., 2018). The probes were amplified with primers TaAGL6RNAiPF/TaAGL6T7-R (henceforth referred to as the 'antisense probe') and TaAGL6T7-F/TaAGL6RNAiPR (henceforth referred to as the 'sense probe') (Table S1).

Generating transgenic plants

To construct the overexpression vectors, one pair of primers TaAGL6OF/TaAGL6OR (Table S1) was designed to amplify the coding region, because of the identical sequence after the ATG and before the TGA in three genes (Fig. S1). The PCR products were then cloned into pMD18-T vectors, three different cDNAs were selected by sequencing different clones and the encoding *TaAGL6* cDNAs were cloned into the pCAMBIA1301 vectors (TaKaRa) with *Nco*I and *Bgl*II sites under the control of the 35S promoter. The dsRNAi vector was constructed according to a previous study (Li et al., 2010). Wheat was transformed via gene gun bombardment, according to a previous study (Zhang et al., 2015). Transformation of *Arabidopsis* was mediated by *Agrobacterium tumefaciens* GV3101.

Histological analyses and scanning electron microscopy

The materials were fixed in FAA at 4°C overnight, dehydrated in graded ethanol then xylene. They were then embedded in Paraplast Plus (Sigma-Aldrich) and cut into 8 µm sections, which were stained with 0.2% Toluidine Blue and photographed using a Nikon E600 microscope and a Nikon DXM1200 digital camera. Scanning electron microscopy (SEM) images were obtained using a JSM-6360LV (JEOL) scanning electron microscope, as described previously (Liu et al., 2016).

Y2H assay

Y2H assays were performed using the GAL4-based two-hybrid system (Clontech). Self-activation assays of three TaAGL6, TaAP3, TaAG and TaMADS13 were performed according to the protocol. The coding sequence (CDS) of three *TaAGL6* genes was cloned in the frame of pGADT7-Rec to generate pGAD-Preys. The coding regions of *TaAP3*, *TaAG* and *TaMADS13* were cloned in the frame of pGBKT7 to generate pGBK-Baits. The different combinations of pGAD-Preys and pGBK-Baits were co-transformed into Y2HGold yeast cells (Clontech). Positive clones on SD/-Trp/-Leu solid medium were transferred to SD/-Trp-Leu-His or SD/-Trp-Leu-His-Ade liquid medium to detect the interactions. Clones harboring pGADT7-*TaAGL6* and pGBKT7 were used as the negative control. The primers are listed in Table S1.

BiFC assay

BiFC vectors pSPYNE and pSPYCE were used to construct nYFP-TaAGL6-A/B/D, TaAP3-cYFP, TaAG-cYFP and TaMADS13-Cyfp, with the one-step cloning kit (Yeasen Biotech). *Agrobacterium* GV3101 cells harboring different nYFP-TaAGL6 and different cYFP constructs were infiltrated into *N. benthamiana* leaves. YFP fluorescence was observed under a confocal laser scanning microscope (Olympus FV10 ASW). Three independent *N. benthamiana* leaves were observed for the analysis of every interaction.

Protein expression and purification and western blot analysis

The partial cDNA (1-507 bp) of *TaAGL6-B* was amplified with the primers TaAGL6-BGSTF and TaAGL6-BGSTR (Table S1), and inserted into *Eco*RI and *Xho*I sites of the pGEX-6p-1 vector to express the fusion protein glutathione-*S*-transferase (GST)-TaAGL6-B. The construct was then introduced into BL21 (DE3) pLysS *E. coli* cells. Positive clones were cultured in Luria-Bertani (LB) medium containing 50 mg/ml ampicillin at 37°C to OD_{600}=0.6. Expression of the fusion protein was induced by adding 1 mM isopropyl β-D-1-thiogalactopyranoside. The fusion proteins were purified using glutathione-agarose beads (Sangon Biotech), according to the manufacturer's instructions.

The purified proteins were separated on 12% SDS-PAGE gels and transferred to a polyvinylidene difluoride (0.45 µm) membrane (Millipore, cat: IPVH00010F). After blocking for 3 h in Tris-buffered saline Tween (TBST) with 5% nonfat milk, the membrane was washed with TBST three times (5 min each time) and incubated with the GST antibody at a dilution of 1:1000 (D190101, Sangon Biotech) at 4°C overnight. Secondary goat anti-mouse IgG conjugated with horseradish peroxidase (D110087, Sangon Biotech) was then incubated with the membrane for 2 h at a dilution of 1:5000. The target protein bands were visualized using a chemiluminescence reagent (Beyotime Biotechnology) (Song et al., 2018).

Electrophoretic mobility shift assay

The fragments including the CArG cis-element in the *TaAP3* promoter were amplified using PCR with biotin-labeled or non-labeled primers (Table S1). The biotin-labeled DNA probes were incubated with the TaAGL6-B-GST protein, and competing experiments were performed by adding excess non-labeled probes. Biotin-labeled probes incubated with GST protein served as the negative control. EMSA assays were performed using the LightShift Chemiluminescent EMSA Kit (20148, Thermo), according to the manufacturer's instructions. Briefly, the reaction mixture [in 20 µl: 10 µg purified fused protein or GST, 100 fmol biotin end-labeled probes, 2 µl 10× binding buffer, 1 µl of 1 µg/µl poly (dI·dC), 1 µl 50% glycerol, 1 µl 1% NP-40, 1 µl of 1 M KCl, 1 µl of 100 mM $MgCl_2$, 0.5 µl of 200 mM EDTA and double-distilled water] was incubated for 30 min at room temperature for the binding reaction and electrophoresed on a 10% native polyacrylamide gel. The proteins were then transferred to a nylon membrane (S4056, Millipore) in 0.5× TBE buffer at 380 mA for 45-60 min, and the binding between the proteins and biotin-labeled probes was detected by chemiluminescence (Feng et al., 2014).

Y1H analysis

For the Y1H assay, three copies of the CArG element were cloned into the pAbAi vector to create the bait construct. The CDS of three *TaAGL6* genes were fused to the GAL4 AD in the pGADT7 vector to generate the prey constructs AD-*TaAGL6-A*, AD-*TaAGL6-B* and AD-*TaAGL6-D*. The prey vector and the empty vector (AD), serving as the negative control, were then transformed separately into yeast cells containing bait constructs, with the primers TaAP3F/TaAP3R and Mut TaAP3F/Mut TaAP3R (Table S1). The transformed yeast cells were diluted with a 10× dilution series and dotted on the SD plates lacking Leu and Ura with 200 ng/ml (optimized according to the protocol) Aureobasidin A. The binding between prey protein and bait sequence is judged by the growth of cells harboring bait construct and prey construct.

Transient expression assay

To generate reporter construct, a 1746 bp region upstream of TaAP3-B start codon was amplified and cloned into a pGreenII 0800-LUC vector (Hellens et al., 2005). To create an effecter construct, TaAGL6-B CDS were cloned into pGreenII 62-SK vector (Hellens et al., 2005). The recombinant effecter and reporter plasmids were transfected into *A. tumefaciens* strain GV3101 (pGreenII series holding psoup plasmid) separately and co-infected into tobacco leaves. A dual-luciferase reporter assay system (Promega) was used to measure firefly LUC and renilla luciferase (REN) activities. The REN gene under the control of the CaMV 35S promoter and the LUC gene were in the pGreenII 0800-LUC vector (Hellens et al., 2005). Relative REN activity was used as an internal control, and LUC/REN ratios were calculated. At least three assay measurements were performed for each assay.

Co-immunoprecipitation assays

The HA-tag vector Gold and GFP-tag vector pCAMBIA1302 were used for co-immunoprecipitation analysis. Full-length CDSs of TaAGL6-B, TaAP3, TaAG and TaMADS13 were amplified and inserted into the tag vectors.

Agrobacterium strains carrying TaAP3-GFP, TaAG-GFP or TaMADS13-GFP were co-infiltrated into tobacco leaves with an Agrobacterium strain carrying TaAGL6-B-HA and P19 silencer, respectively. After 3 days, leaves were harvested, frozen in liquid nitrogen and homogenized with protein extraction buffer. Homogenates were centrifuged (14,000 ***g***) for 15 min at 4° C. The expressed HA-TaAGL6 and TaAP3-GFP, TaAG-GFP, TaMADS13-GFP or GFP proteins, were immunoprecipitated with GFP-Trap MA beads (ChromoTek) at 4°C for 2 h. The immunoprecipitated proteins were washed four times with the lysis buffer and then eluted by boiling for 5 min with 2× loading buffer. Immunoblots were detected by performing western blotting with an anti-GFP antibody (D190750-0100; Sangon; 1:1000), an anti-HA antibody (AH158; Beyotime; 1:1000) and the secondary goat anti-mouse IgG conjugated with horseradish peroxidase (D110087, Sangon Biotech; 1:5000). Total proteins (50 mg) extracted from tobacco leaves co-expressing HA-TaAGL6 and TaAP3-GFP, TaAG-GFP, TaMADS13-GFP or GFP were used as input control (Li et al., 2019). Western blotting was carried out as described above.

Statistical analyses

All statistical analyses were performed using Student's *t*-test in the Statistical Product and Service Solutions (SPSS) software. The differences were examined using Student's *t*-test and the significance level was set at 0.05 (P<0.05).

Accession numbers

TaAGL6-A, *TaAGL6-B* and *TaAGL6-D* are in the GRAMENE database (www.gramene.org) under *TraesCS6A02G259000*, *TraesCS6B02G286400* and *TraesCS6D02G240200*, respectively.

Acknowledgements

We appreciate the kind help from Dr Dejun Han and Dr Yu Wang at Northwest A&F University (Shaanxi, China).

Competing interests

The authors declare no competing or financial interests.

Author contributions

Conceptualization: H.L., Z.K.; Methodology: C.G., D.Z.; Investigation: Y.S., J.L., W. Liang, Y.D., R.F., W. Li, C.F.; Writing - original draft: H.L.; Supervision: H.L., Z.K.; Project administration: H.L.; Funding acquisition: H.L.

Funding

This work was supported by the National Natural Science Foundation of China (31571657), by the Program of Introducing Talents of Innovative Discipline to Universities (Project 111) from the State Administration of Foreign Experts Affairs (B18042), and by the China Scholarship Council (201806305041).

Supplementary information

Supplementary information available online at
http://dev.biologists.org/lookup/doi/10.1242/dev.177527.supplemental

References

Ambrose, B. A., Lerner, D. R., Ciceri, P., Padilla, C. M., Yanofsky, M. F. and Schmidt, R. J. (2000). Molecular and genetic analyses of the Silky1 gene reveal conservation in floral organ specification between eudicots and monocots. *Mol. Cell* **5**, 569-579. doi:10.1016/S1097-2765(00)80450-5

Appels, R., Eversole, K., Feuillet, C., Keller, B., Rogers, J., Stein, N., Pozniak, C. J., Stein, N., Choulet, F., Distelfeld, A. et al. (2018). Shifting the limits in wheat research and breeding using a fully annotated reference genome. *Science* **361**, eaar7191. doi:10.1126/science.aar7191

Becker, A. and Theissen, G. (2003). The major clades of MADS-box genes and their role in the development and evolution of flowering plants. *Mol. Phylogenet. Evol.* **29**, 464-489. doi:10.1016/S1055-7903(03)00207-0

Coen, E. S. and Meyerowitz, E. M. (1991). The war of the whorls: genetic interactions controlling flower development. *Nature* **353**, 31-37. doi:10.1038/353031a0

Cui, R., Han, J., Zhao, S., Su, K., Wu, F., Du, X., Xu, Q., Chong, K., Theißen, G. and Meng, Z. (2010). Functional conservation and diversification of class E floral homeotic genes in rice (Oryza sativa). *Plant J.* **61**, 767-781. doi:10.1111/j.1365-313X.2009.04101.x

Ditta, G., Pinyopich, A., Robles, P., Pelaz, S. and Yanofsky, M. F. (2004). The SEP4 gene of Arabidopsis thaliana functions in floral organ and meristem identity. *Curr. Biol.* **14**, 1935-1940. doi:10.1016/j.cub.2004.10.028

Dreni, L. and Zhang, D. B. (2016). Flower development: the evolutionary history and functions of the AGL6 subfamily MADS-box genes. *J. Exp. Bot.* **67**, 1625-1638. doi:10.1093/jxb/erw046

Dreni, L., Jacchia, S., Fornara, F., Fornari, M., Ouwerkerk, P. B. F., An, G., Colombo, L. and Kater, M. M. (2007). The D-lineage MADS-box gene OsMADS13 controls ovule identity in rice. *Plant J.* **52**, 690-699. doi:10.1111/j.1365-313X.2007.03272.x

Dreni, L., Pilatone, A., Yun, D. P., Erreni, S., Pajoro, A., Caporali, E., Zhang, D. B. and Kater, M. M. (2011). Functional analysis of all AGAMOUS subfamily members in rice reveals their roles in reproductive organ identity determination and meristem determinacy. *Plant Cell* **23**, 2850-2863. doi:10.1105/tpc.111.087007

Duan, Y. L., Xing, Z., Diao, Z. J., Xu, W. Y., Li, S. P., Du, X. Q., Wu, G. H., Wang, C. L., Lan, T., Meng, Z. et al. (2012). Characterization of Osmads6-5, a null allele, reveals that OsMADS6 is a critical regulator for early flower development in rice (Oryza sativa L.). *Plant Mol. Biol.* **80**, 429-442. doi:10.1007/s11103-012-9958-2

Feng, C.-Z., Chen, Y., Wang, C., Kong, Y.-H., Wu, W.-H. and Chen, Y.-F. (2014). Arabidopsis RAV1 transcription factor, phosphorylated by SnRK2 kinases, regulates the expression of ABI3, ABI4, and ABI5 during seed germination and early seedling development. *Plant J.* **80**, 654-668. doi:10.1111/tpj.12670

Feng, N., Song, G., Guan, J., Chen, K., Jia, M., Huang, D., Wu, J., Zhang, L., Kong, X., Geng, S. et al. (2017). Transcriptome profiling of wheat inflorescence development from spikelet initiation to floral patterning identified stage-specific regulatory genes. *Plant Physiol.* **174**, 1779-1794. doi:10.1104/pp.17.00310

Gao, X., Liang, W., Yin, C., Ji, S., Wang, H., Su, X., Guo, C., Kong, H., Xue, H. and Zhang, D. (2010). The SEPALLATA-like gene OsMADS34 is required for rice inflorescence and spikelet development. *Plant Physiol.* **153**, 728-740. doi:10.1104/pp.110.156711

Gu, X., Wang, Y. and He, Y. (2013). Photoperiodic regulation of flowering time through periodic histone deacetylation of the florigen gene FT. *PLoS Biol.* **11**, e1001649. doi:10.1371/journal.pbio.1001649

Hellens, R. P., Allan, A. C., Friel, E. N., Bolitho, K., Grafton, K., Templeton, M. D., Karunairetnam, S., Gleave, A. P. and Laing, W. A. (2005). Transient expression vectors for functional genomics, quantification of promoter activity and RNA silencing in plants. *Plant Methods* **1**, 13. doi:10.1186/1746-4811-1-13

Hsu, W.-H., Yeh, T.-J., Huang, K.-Y., Li, J.-Y., Chen, H.-Y. and Yang, C.-H. (2014). AGAMOUS-LIKE13, a putative ancestor for the E functional genes, specifies male and female gametophyte morphogenesis. *Plant J.* **77**, 1-15. doi:10.1111/tpj.12363

Hu, L., Liang, W., Yin, C., Cui, X., Zong, J., Wang, X., Hu, J. and Zhang, D. (2011). Rice MADS3 regulates ROS homeostasis during late anther development. *Plant Cell* **23**, 515-533. doi:10.1105/tpc.110.074369

Huang, X., Effgen, S., Meyer, R. C., Theres, K. and Koornneef, M. (2012). Epistatic natural allelic variation reveals a function of AGAMOUS-LIKE6 in axillary bud formation in Arabidopsis. *Plant Cell* **24**, 2364-2379. doi:10.1105/tpc.112.099168

Jeon, J., Jang, S., Lee, S., Jung, K., Nam, J., Kim, C., Lee, S., Chung, Y., Kim, S., Lee, Y. et al. (2000). Leafy hull sterile 1 is a homeotic mutation in a rice MADS Box gene affecting rice flower development. *Plant Cell* **12**, 871-884. doi:10.1105/tpc.12.6.871

Kobayashi, K., Maekawa, M., Miyao, A., Hirochika, H. and Kyozuka, J. (2010). PANICLE PHYTOMER2 (PAP2), encoding a SEPALLATA subfamily MADS-box protein, positively controls spikelet meristem identity in rice. *Plant Cell Physiol.* **51**, 47-57. doi:10.1093/pcp/pcp166

Kobayashi, K., Yasuno, N., Sato, Y., Yoda, M., Yamazaki, R., Kimizu, M., Yoshida, H., Nagamura, Y. and Kyozuka, J. (2012). Inflorescence meristem identity in rice is specified by overlapping functions of three AP1/FUL-Like MADS Box genes and PAP2, a SEPALLATA MADS Box gene. *Plant Cell* **24**, 1848-1859. doi:10.1105/tpc.112.097105

Koo, S. C., Bracko, O., Park, M., Schwab, R., Chun, H., Park, K., Seo, J., Grbic, V., Balasubramanian, S., Schmid, M. et al. (2010). Control of lateral organ development and flowering time by the Arabidopsis thaliana MADS-box Gene AGAMOUS-LIKE6. *Plant J.* **62**, 807-816. doi:10.1111/j.1365-313X.2010.04192.x

Li, H., Liang, W., Jia, R., Yin, C., Zong, J., Kong, H. and Zhang, D. (2010). The AGL6-like gene OsMADS6 regulates floral organ and meristem identities in rice. *Cell Res.* **20**, 299-313. doi:10.1038/cr.2009.143

Li, H.-F., Han, Y., Liu, M.-J., Wang, B.-H., Su, Y.-L. and Sun, Q.-X. (2016). Expression patterns of *MADS-box* genes related to flower development of wheat. *Acta Agron Sin.* **42**, 1067-1073. doi:10.3724/SP.J.1006.2016.01067

Li, H., Liang, W., Hu, Y., Zhu, L., Yin, C., Xu, J., Dreni, L., Kater, M. M. and Zhang, D. (2011a). Rice MADS6 interacts with the floral homeotic genes SUPERWOMAN1, MADS3, MADS58, MADS13, and DROOPING LEAF in specifying floral organ identities and meristem fate. *Plant Cell* **23**, 2536-2552. doi:10.1105/tpc.111.087262

Li, H., Liang, W., Yin, C., Zhu, L. and Zhang, D. (2011b). Genetic interaction of OsMADS3, DROOPING LEAF, and OsMADS13 in specifying rice floral organ identities and meristem determinacy. *Plant Physiol.* **156**, 263-274. doi:10.1104/pp.111.172080

Li, D., Zhang, H., Mou, M., Chen, Y., Xiang, S., Chen, L. and Yu, D. (2019). Arabidopsis class II TCP transcription factors integrate with the FT-FD module to control flowering. *Plant Physiol.* **181**, 97-111. doi:10.1104/pp.19.00252

Lin, X., Wu, F., Du, X., Shi, X., Liu, Y., Liu, S., Hu, Y., Theißen, G. and Meng, Z. (2014). The pleiotropic SEPALLATA-like gene OsMADS34 reveals that the 'empty glumes' of rice (Oryza sativa) spikelets are in fact rudimentary lemmas. *New Phytol.* **202**, 689-702. doi:10.1111/nph.12657

Liu, M., Li, H., Su, Y., Li, W. and Shi, C. (2016). G1/ELE functions in the development of rice lemmas in addition to determining identities of empty glumes. *Front. Plant Sci.* **7**, 1006. doi:10.3389/fpls.2016.01006

Livak, K. J. and Schmittgen, T. D. (2001). Analysis of relative gene expression data using real-time quantitative PCR and the 2(T)(-Delta Delta C) method. *Methods* **25**, 402-408. doi:10.1006/meth.2001.1262

Murai, K. (2013). Homeotic genes and the ABCDE model for floral organ formation in wheat. *Plants (Basel)* **2**, 379-395. doi:10.3390/plants2030379

Nagasawa, N., Miyoshi, M., Sano, Y., Satoh, H., Hirano, H., Sakai, H. and Nagato, Y. (2003). SUPERWOMAN1 and DROOPING LEAF genes control floral organ identity in rice. *Development* **130**, 705-718. doi:10.1242/dev.00294

Ohmori, S., Kimizu, M., Sugita, M., Miyao, A., Hirochika, H., Uchida, E., Nagato, Y. and Yoshida, H. (2009). MOSAIC FLORAL ORGANS1, an AGL6-like MADS box gene, regulates floral organ identity and meristem fate in rice. *Plant Cell* **21**, 3008-3025. doi:10.1105/tpc.109.068742

Paolacci, A. R., Tanzarella, O. A., Porceddu, E., Varotto, S. and Ciaffi, M. (2007). Molecular and phylogenetic analysis of MADS-box genes of MIKC type and chromosome location of SEP-like genes in wheat (Triticum aestivum L.). *Mol. Genet. Genomics* **278**, 689-708. doi:10.1007/s00438-007-0285-2

Pelaz, S., Ditta, G. S., Baumann, E., Wisman, E. and Yanofsky, M. F. (2000). B and C floral organ identity functions require SEPALLATA MADS-box genes. *Nature* **405**, 200-203. doi:10.1038/35012103

Reinheimer, R. and Kellogg, E. A. (2009). Evolution of AGL6-like MADS Box genes in Grasses (Poaceae): ovule expression is ancient and palea expression is new. *Plant Cell* **21**, 2591-2605. doi:10.1105/tpc.109.068239

Rijpkema, A. S., Zethof, J., Gerats, T. and Vandenbussche, M. (2009). The petunia AGL6 gene has a SEPALLATA-like function in floral patterning. *Plant J.* **60**, 1-9. doi:10.1111/j.1365-313X.2009.03917.x

Schwarz-Sommer, Z., Huijser, P., Nacken, W., Saedler, H. and Sommer, H. (1990). Genetic control of flower development by homeotic genes in Antirrhinum majus. *Science* **250**, 931-936. doi:10.1126/science.250.4983.931

Seok, H.-Y., Park, H.-Y., Park, J.-I., Lee, Y.-M., Lee, S.-Y., An, G. and Moon, Y.-H. (2010). Rice ternary MADS protein complexes containing class B MADS heterodimer. *Biochem. Biophys. Res. Commun.* **401**, 598-604. doi:10.1016/j.bbrc.2010.09.108

Shewry, P. R. (2009). Wheat. *J. Exp. Bot.* **60**, 1537-1553. doi:10.1093/jxb/erp058

Song, H., Tao, Y., Ni, N. N., Zhou, X. W., Xiong, J. S., Zeng, X. S., Xu, X. L., Qi, J. L. and Sun, J. F. (2018). miR-128 targets the CC chemokine ligand 18 gene (CCL18) in cutaneous malignant melanoma progression. *J. Dermatol. Sci.* **91**, 317-324. doi:10.1016/j.jdermsci.2018.06.011

Tao, J., Liang, W., An, G. and Zhang, D. (2018). OsMADS6 controls flower development by activating rice FACTOR OF DNA METHYLATION LIKE1. *Plant Physiol.* **177**, 713-727. doi:10.1104/pp.18.00017

Theißen, G. (2001). Plant biology-floral quartets. *Nature* **409**, 469-471. doi:10.1038/35054172

Thompson, B., Bartling, L., Whipple, C., Hall, D., Sakai, H., Schmidt, R. and Hake, S. (2009). bearded-ear encodes a MADS box transcription factor critical for maize floral development. *Plant Cell* **21**, 2578-2590. doi:10.1105/tpc.109.067751

Waddington, S., Cartwright, P. and Wall, P. (1983). A quantitative scale of spike initial and pistil development in barley and wheat. *Ann. Bot.* **51**, 119-130. doi:10.1093/oxfordjournals.aob.a086434

Whipple, C. J., Ciceri, P., Padilla, C. M., Ambrose, B. A., Bandong, S. L. and Schmidt, R. J. (2004). Conservation of B-class floral homeotic gene function between maize and Arabidopsis. *Development* **131**, 6083-6091. doi:10.1242/dev.01523

Wu, F., Shi, X., Lin, X., Liu, Y., Chong, K., Theißen, G. and Meng, Z. (2017). The ABCs of flower development: mutational analysis of AP1/FUL-like genes in rice provides evidence for a homeotic (A)-function in grasses. *Plant J.* **89**, 310-324. doi:10.1111/tpj.13386

Yadav, S. R., Khanday, I., Majhi, B. B., Veluthambi, K. and Vijayraghavan, U. (2011). Auxin-responsive OsMGH3, a common downstream target of OsMADS1 and OsMADS6, controls rice floret fertility. *Plant Cell Physiol.* **52**, 2123-2135. doi:10.1093/pcp/pcr142

Yamaguchi, T., Nagasawa, N., Kawasaki, S., Matsuoka, M., Nagato, Y. and Hirano, H.-Y. (2004). The YABBY gene DROOPING LEAF regulates carpel specification and midrib development in Oryza sativa. *Plant Cell* **16**, 500-509. doi:10.1105/tpc.018044

Yamaguchi, T., Lee, D., Miyao, A., Hirochika, H., An, G. and Hirano, H.-Y. (2006). Functional diversification of the two C-class MADS box genes OSMADS3 and OSMADS58 in Oryza sativa. *Plant Cell* **18**, 15-28. doi:10.1105/tpc.105.037200

Yoo, S. K., Hong, S. M., Lee, J. S. and Ahn, J. H. (2011a). A genetic screen for leaf movement mutants identifies a potential role for AGAMOUS-LIKE 6 (AGL6) in circadian-clock control. *Mol. Cells* **31**, 281-287. doi:10.1007/s10059-011-0035-5

Yoo, S. K., Wu, X. L., Lee, J. S. and Ahn, J. H. (2011b). AGAMOUS-LIKE 6 is a floral promoter that negatively regulates the FLC/MAF clade genes and positively regulates FT in Arabidopsis. *Plant J.* **65**, 62-76. doi:10.1111/j.1365-313X.2010.04402.x

Zhang, J. A., Nallamilli, B. R., Mujahid, H. and Peng, Z. H. (2010). OsMADS6 plays an essential role in endosperm nutrient accumulation and is subject to epigenetic regulation in rice (Oryza sativa). *Plant J.* **64**, 604-617. doi:10.1111/j.1365-313X.2010.04354.x

Zhang, K., Liu, J. X., Zhang, Y., Yang, Z. M. and Gao, C. X. (2015). Biolistic genetic transformation of a wide range of chinese elite wheat (Triticum aestivum L.) varieties. *J. Genet. Genomics* **42**, 39-42. doi:10.1016/j.jgg.2014.11.005